Anal Bioanal Chem
DOI 10.1007/s00216-016-9330-5

RAPID COMMUNICATION

# Spherical silver nanoparticles in the detection of thermally denatured collagens

**Manuel Ahumada**[1,2] · **Sarah McLaughlin**[1] · **Natalia L. Pacioni**[3] · **Emilio I. Alarcon**[1,4]

Received: 11 November 2015 / Revised: 27 December 2015 / Accepted: 12 January 2016


**Abstract** We have developed a rapid colorimetric method to determine the concentration of denatured collagen in solution, which is based on the collagen-silver nanoparticle corona formation. Using the proposed method, the lowest detectable concentration of denatured collagen protein in a solution of pure collagen was 14.7, 8.5, and 8.6 μg $mL^{-1}$ for porcine (PCOL), rat tail (RCOL), and type I human recombinant (HCOL) collagen, respectively.

**Keywords** Collagen · Nanoparticles/Nanotechnology · Surface plasmon band

**Electronic supplementary material** The online version of this article (doi:10.1007/s00216-016-9330-5) contains supplementary material, which is available to authorized users.

✉ Natalia L. Pacioni
nataliap@fcq.unc.edu.ar

✉ Emilio I. Alarcon
ealarcon@ottawaheart.ca

[1] Bio-nanomaterials Chemistry and Engineering Laboratory, Division of Cardiac Surgery, University of Ottawa Heart Institute, 40 Ruskin Street, Rm H5229, Ottawa, Ontario K1Y 4W7, Canada

[2] Laboratorio de Cinética y Fotoquímica, Departamento de Ciencias del Ambiente-Facultad de Química y Biología, Universidad de Santiago de Chile, Avenida Libertador Bernardo O´higgins 3363, 8370071 Santiago, Chile

[3] Departamento de Química Orgánica-Facultad de Ciencias Químicas, INFIQC-CONICET and Universidad Nacional de Córdoba, Haya de la Torre y Medina Allende s/n, X5000HUA, Ciudad Universitaria, 5000 Córdoba, Argentina

[4] Department of Biochemistry, Microbiology and Immunology, Faculty of Medicine, University of Ottawa, Ottawa, Ontario K1Y 4W7, Canada

The interactions between proteins and metallic nanoparticles, including silver, play a pivotal role in the biological activity of nanosized materials, although the majority of mechanisms governing these interactions remain unknown [1–5]. Protein–nanoparticle interactions can be detected in solution because changes in the noble metal nanoparticle surface composition are macroscopically perceivable as shifts in the surface plasmon band (SPB) which, for example, can result in a change of solution color [6]. For the specific case of silver nanoparticles (AgNPs), without low molecular weight protecting agents, it has been described that proteins like human and bovine serum albumins, lysozyme, and collagen can act as protecting agents for the nanoparticle surface [7–13]. Further, recent research by our team has found that type I porcine collagen (PCOL) is an efficient capping agent for nascent $Ag^0$, which nucleate to form spherical AgNPs [14].

In the present work, we observed that the addition of 34 μg $mL^{-1}$ of native, non-denatured, (nPCOL) or denatured (dPCOL) PCOL (≈ 0.1 μM) to a colloidal solution of citrate capped AgNPs, 6.3 ± 0.4 nm, resulted in a fast (<30 s) ≈ 12 nm red shift of the SPB maximum position from 394 to 405 nm or 407 nm, respectively, see Fig. 1 left top inset ($p < 0.05$ ANOVA test, see SI). This change occurs with an increase in the full width at a half medium (FWHM) value (Fig. 1, left bottom inset, $p < 0.05$ ANOVA test), and remains practically unchanged for up to 2 h, see Fig. 1 left. Interestingly, when we monitored the intensity of absorption at the SPB, see Fig. 1 right, we observed that the samples containing nCOL gradually formed a precipitate with a corresponding decrease in the SPB absorption of up to 50 % ($p < 0.05$ ANOVA test). In contrast, samples containing thermally dCOL, by pre-incubating collagen at 95 °C for 5 min, did not show a statistically significant change in the SPB for the 2-h duration of the assay ($p > 0.05$ ANOVA test). Similar results

Published online: 04 February 2016

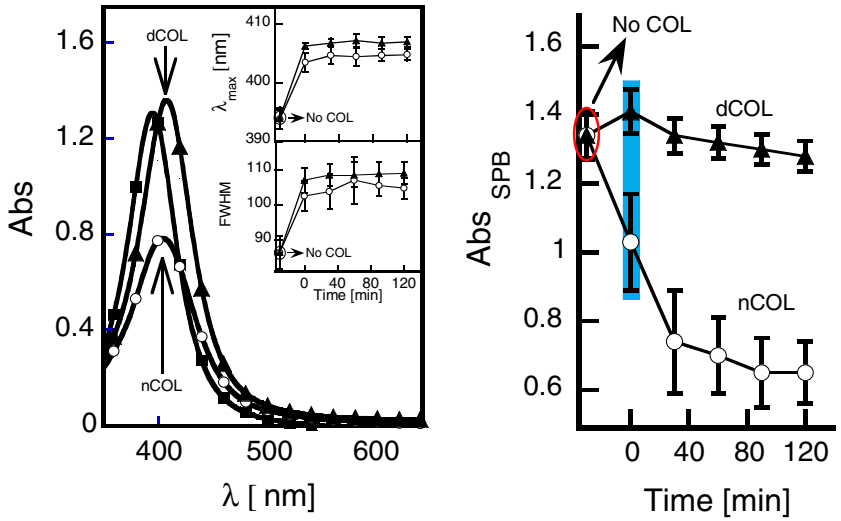


**Fig. 1** **(Left)** Effect of adding PCOL, 34 μg $mL^{-1}$ to a solution of colloidal citrate capped AgNPs. Spectra show the SPB before (squares), and after the addition of nPCOL (open circles ) or dPCOL (filled triangles) collagen. Inset: Top, shows the changes on the SPB maximum position before and after adding collagen. Bottom, changes in the FWHM of the AgNPs measured before and after adding collagen. Note that the first point after the addition of collagen was measured within 30 s. **(Right)** Change in the SPB absorption maxima for AgNPs measured before and after adding 34 μg $mL^{-1}$ of type I collagen either nCOL (open circles) or dCOL (filled triangles). The plasmon intensity for AgNPs before adding collagen has also been included in the plot, denoted with an arrow, but the absorbance was measured at 397 nm. The blue highlighted region corresponds to the first point measured after adding collagen (within 30 s). Error bars correspond to the standard deviation of the experimental data, which was calculated by performing experiments with three different batches of AgNPs in duplicate (N = 6). All measurements were carried out at room temperature

were observed at 4 and 37 °C [see Electronic Supplementary Material (ESM), Fig. S1], which suggests that the formation of the nanoparticle–protein composite, and not the solution temperature, dictates the resulting stability of the AgNPs–collagen complex.

The observed differences in protein–AgNP interaction between the nCOL and dCOL cannot be attributed to protein crosslinking (see ESM, Fig. S2) and must be directly linked to the loss of protein conformation post-thermal treatment of the sample (see ESM, Fig. S3). Therefore, we have harnessed the difference in collagen–AgNP interaction stability between native and denatured protein and developed an efficient method to determine the amount of thermally dCOL in solution. The presented method is fast, reproducible, highly sensitive, and inexpensive compared with other approaches, such as the use of angular displacement techniques and measurement of dielectric properties [15–17]. The main steps of our method are summarized in Scheme 1.

Figure 2A contains representative AgNPs-SPB spectra for the supernatant after the addition of PCOL (total concentration nPCOL + dPCOL: 34 μg $mL^{-1}$), in which the intensity of SPB absorption increases with the amount of thermally dPCOL in solution. When the concentration of dCOL is zero, the supernatant will show no absorption at the AgNPs-SPB wavelength. Figure 2B includes the plots of SPB absorbance versus protein concentration for different species of type I collagen including porcine, rat tail (RCOL), and recombinant human collagen (HCOL). The amount of denatured protein in solution ranged from 4.25 to 34 μg $mL^{-1}$, using a total protein content (nCOL + dCOL) of 34 μg $mL^{-1}$. Note that for PCOL and RCOL collagen the maximum wavelength of absorption for the AgNPs-collagen system was found at 407 nm, whereas for HCOL the wavelength of maximal absorption was 403 nm (see ESM, Fig. S4).

Another interesting observation was that the profile of absorption versus collagen concentration, shown in Fig. 2B, has a nonlinear relationship that could indicate the formation of a corona arrangement around the AgNPs. Protein–AgNP interactions with a corona arrangement occur, in principle, through a multi-step regime [18] such that after the initial protein adsorption onto the nanoparticle layer, subsequent layers will form around this first one, rendering an onion-like protein adsorption on the nanoparticle surface [19]. Although the number of proteins per nanoparticle within the layers will exclusively depend of the chosen protein, our cumulative data shows good reproducibility within AgNPs batches and experiments (see ESM). Thus, our next step was to plot the absorption data shown in Fig. 2B versus the square of the denatured protein concentration.

Figure 3 shows the best linear fit for the plot of absorption ($Abs_{407}$) versus the square of the dCOL concentration ($R^2 > 0.97$, and $\chi^2 < 0.02$), which rendered limits of detections (LOD, defined as $3.3s_B/m$ where $s_B$ is estimated as the residual

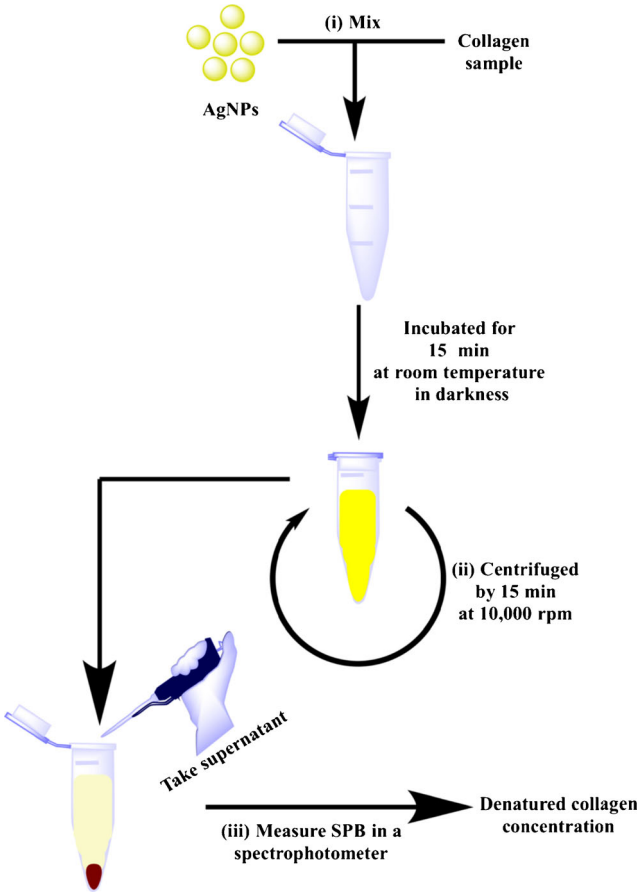


**Scheme 1** Simplified experimental procedure for determining the content of dCOL using citrate capped AgNPs. Main steps are as follows from top to bottom: (i) colloidal solution of AgNPs is mixed with the collagen sample (nCOL + dCOL) in a ratio of 1:1 v/v (AgNPs:COL), incubated for 15 min and protected from light; (ii) this solution is centrifuged for 15 min at 10,000 rpm; (iii) the supernatant (which contains dCOL + AgNPs) is removed and measured using a spectrophotometer (≈407 nm). The amount of dCOL in the sample is determined by interpolating the absorbance reading using a calibration curve of absorbance versus dCOL content

standard deviation and *m* is the slope of the linear fit, Supplementary Table S1) of 14.7, 8.5, and 8.6 μg $mL^{-1}$ for dPCOL, dRCOL, and dHCOL, respectively. Note that the upper concentration limit was determined as 34, 21, and 25 μg $mL^{-1}$, respectively, for each collagen type as mentioned above. Finally, we assessed the capability of our method to determine the denatured collagen concentration in two 'unknown' samples spiked with 30 ± 1 μg $mL^{-1}$ of dRCOL or dHCOL. For these two samples, we detected 28 ± 2 of dRCOL and 26 ± 1 μg $mL^{-1}$ of dHCOL, which represented acceptable recoveries of 93 % and 87 %, respectively.

In addition to the advantages described above, this approach is attractive because it avoids the use of an extra reagent and relies only on the specific interaction between

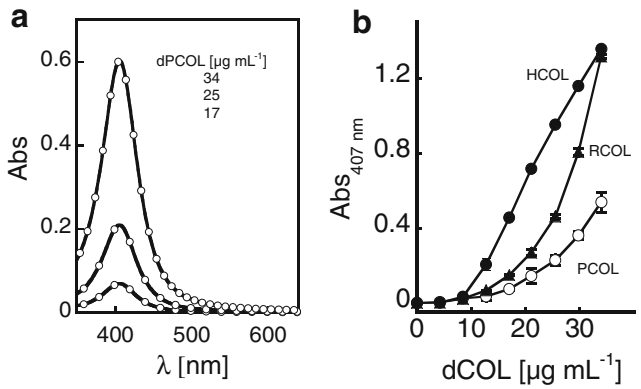


**Fig. 2** **(A)** Representative absorption spectra for AgNPs measured in the supernatant post centrifugation, see main text and Scheme 1, detected at different dPCOL concentrations as indicated in the plot. **(B)** Absorbance at the maximum wavelength for the AgNPs-collagen measured in the supernatant as a function of the dCOL concentration in solution. Note that forall the experiments shown in this figure, total collagen concentration (dCOL + nCOL), was kept as 34 μg $mL^{-1}$. Measurements were performed with three different collagen species: dPCOL (○), dRCOL (▲) and dHCOL (●). Error bars correspond to the standard deviation of the experimental data, whic was calculated by performing experiments with three different batches of AgNPs in duplicate (N = 6). All measurements were carried out at room temperature

AgNPs and COL to determine dCOL. However, the versatility and sensibility of our assay could be further improved by coupling our methodology to, for example, surface enhanced Raman spectroscopy (SERS) [20] and/or by using fluorescence mediated enhancement from AgNPs plasmon similar to that recently described by Stobiecka and Chalupa for gold nanoparticles [21, 22].

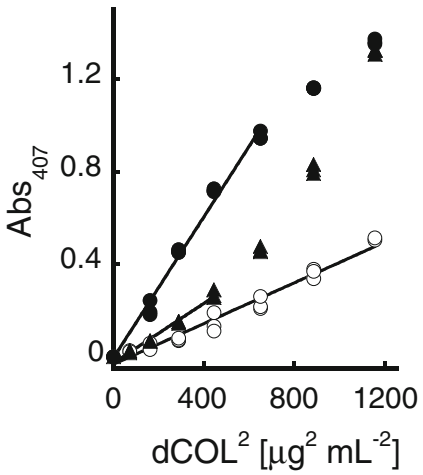


**Fig. 3** Changes on the SPB-absorption plotted against the square of dCOL concentration for PCOL (○), RCOL (▲) and HCOL (●). The lines shown in the plots correspond to the best linear fit obtained in each corresponding case. Data outside the linear range are also shown to visualize the upper limit of the method. All measurements were carried out at room temperature

## Conclusions

In summary, we have developed a new assay to determine the amount of denatured collagen present in a collagen sample solution by using the difference in stability of AgNPs-collagen composites observed upon thermal denaturation of the protein. This assay can be completed in only 30 min without the need of expensive equipment. The proposed assay requires minimal analytical instrumentation, simply a spectrophotometer and a centrifuge, which are available in most laboratories, and allows the detection of quantities on the order of micrograms of denatured collagen for porcine, rat-tail, and human recombinant collagen, respectively.

**Acknowledgments** This work was funded by the Natural Sciences and Engineering Research Council (Discovery RGPIN-2015-06325 to E.I.A.) and start-up grant 1255 UOHI to E.I.A. M.A. thanks the Government of Canada for the Canada-Chile Exchange Leadership Scholarship and CONICYT for a doctoral fellowship (no. 21120182). N.L.P. is a research member of the Consejo Nacional de Investigaciones Científicas y Técnicas (CONICET) of Argentina. The authors thank Professor Eduardo Lissi, USACH-Chile, for his useful comments on the article. Type I recombinant collagen was a kind gift from Professor May Griffith, Linkoping University, Sweden.

**Compliance with ethical standards**

**Conflict of interest** The authors declare that they have no conflict of interest.

## References

1. Cho EC, Zhang Q, Xia Y. The effect of sedimentation and diffusion on cellular uptake of gold nanoparticles. Nat Nanotechnol. 2011;6(6):385–91.
2. Ghosh P, Han G, De M, Kim CK, Rotello VM. Gold nanoparticles in delivery applications. Adv Drug Del Rev. 2008;60(11): 130–1315.
3. Laval JM, Mazeran PE, Thomas D. Nanobiotechnology and its role in the development of new analytical devices. Analyst. 2000;125(1):29–33.
4. Niemeyer CM. Nanoparticles, proteins, and nucleic acids: biotechnology meets materials science. Angew Chem Int Ed Engl. 2001;40(22):4128–58.
5. Saptarshi SR, Duschl A, Lopata AL. Interaction of nanoparticles with proteins: relation to bio-reactivity of the nanoparticle. J Nanobiotechnol. 2013;11:26–37.
6. de Alwis Weerasekera H, Griffith M, Alarcon EI. Biomedical Uses of Silver Nanoparticles: From Roman Wine Cups to Biomedical Devices. In: Alarcon EI, Udekwu K, Griffith M, editors. Silver nanoparticle applications: in the fabrication and design of medical and biosensing devices. UK: Springer International Publishing; 2015. p. 93–125.
7. Alarcon EI, Bueno-Alejo CJ, Noel CW, Stamplecoskie KG, Pacioni NL, Poblete H, et al. Human serum albumin as protecting agent of silver nanoparticles: role of the protein conformation and amine groups in the nanoparticle stabilization. J Nanoparticle Res. 2013;15(1):1–14.
8. Alarcon EI, Udekwu KI, Noel CW, Gagnon LBP, Taylor PK, Vulesevic B, et al. Safety and efficacy of composite collagen-silver nanoparticle hydrogels as tissue engineering scaffolds. Nanoscale. 2015;7(44):18789–98.
9. Cardoso VS, Quelemes PV, Amorin A, Primo FL, Gobo GG, Tedesco AC, et al. Collagen-based silver nanoparticles for biological applications: synthesis and characterization. J Nanobiotechnol. 2014;12:36–44.
10. Eby DM, Schaeublin NM, Farrington KE, Hussain SM, Johnson GR. Lysozyme catalyzes the formation of antimicrobial silver nanoparticles. ACS Nano. 2009;3(4):984–94.
11. Murawala P, Phadnis SM, Bhonde RR, Prasad BL. In situ synthesis of water dispersible bovine serum albumin capped gold and silver nanoparticles and their cytocompatibility studies. Coll Surf B Biointerfaces. 2009;73(2):224–8.
12. Ravindran A, Singh A, Raichur AM, Chandrasekaran N, Mukherjee A. Studies on interaction of colloidal Ag nanoparticles with Bovine Serum Albumin (BSA). Coll Surf B Biointerfaces. 2010;76(1):32–7.
13. Wang B, Seabrook SA, Nedumpully-Govindan P, Chen P, Yin H, Waddington L, et al. Thermostability and reversibility of silver nanoparticle-protein binding. Phys Chem Chem Phys. 2015;17(3): 1728–39.
14. Alarcon EI, Udekwu K, Skog M, Pacioni NL, Stamplecoskie KG, Gonzalez-Bejar M, et al. The biocompatibility and antibacterial properties of collagen-stabilized, photochemically prepared silver nanoparticles. Biomaterials. 2012;33(19):4947–56.
15. Barringer SA, Bircan C. Use of the Dielectric Properties to Detect Protein Denaturation. In: Willert-Porada M, editor. Advances in Microwave and Radio Frequency Processing. Berlin Heidelberg: Springer; 2006. p. 107–18.
16. Chen HH, Wu CM, Chen HW, Tseng KH. Detection of thermal denaturation and renaturation of collagen: optical characteristics using angular displacement-enhanced heterodyne polarimeter. Exp Techniques. 2015. doi:10.1111/ext.12138.
17. Hoemann CD, Sun J, Chrzanowski V, Buschmann MD. A multivalent assay to detect glycosaminoglycan, protein, collagen, RNA, and DNA content in milligram samples of cartilage or hydrogel-based repair cartilage. Anal Biochem. 2002;300(1):1–10.
18. Poblete H, Agarwal A, Thomas SS, Bohne C, Ravichandran R, Phopase J, et al. New insights on peptide–silver nanoparticle interaction: deciphering the role of cysteine and lysine in the peptide sequence. Langmuir. 2016;32(1):265–73.
19. Lynch I, Dawson KA. Protein-nanoparticle interactions. Nano Today. 2008;3(1/2):40–7.
20. Khetani A, Momenpour A, Alarcon EI, Anis H. Hollow core photonic crystal fiber for monitoring leukemia cells using surface enhanced Raman scattering (SERS). Biomed Opt Express. 2015;6(11):4599–609.
21. Stobiecka M, Chalupa A. Modulation of plasmon-enhanced resonance energy transfer to gold nanoparticles by protein survivin channeled-shell gating. J Phys Chem B. 2015;119(41):13227–35.
22. Stobiecka M. Novel plasmonic field-enhanced nanoassay for trace detection of proteins. Biosens Bioelectron. 2014;55:379–85.